

Published in final edited form as:

Retina. 2012 May ; 32(5): 865–876. doi:10.1097/IAE.0b013e318251a3a8.

CHOROIDAL IMAGING USING SPECTRAL-DOMAIN OPTICAL COHERENCE TOMOGRAPHY

Caio V. Regatieri, MD, PhD^{*,†}, Lauren Branchini, BA^{*,‡}, James G. Fujimoto, PhD[§], and Jay S. Duker, MD^{*}

^{*}Department of Ophthalmology, New England Eye Center, Tufts Medical Center, Boston, Massachusetts

[†]Department of Ophthalmology, Federal University of São Paulo, São Paulo, Brazil

[‡]Department of Ophthalmology, Boston University School of Medicine, Boston, Massachusetts

[§]Department of Electrical Engineering and Computer Science, Research Laboratory of Electronics, Massachusetts Institute of Technology, Cambridge, Massachusetts

Abstract

Background—A structurally and functionally normal choroidal vasculature is essential for retinal function. Therefore, a precise clinical understanding of choroidal morphology should be important for understanding many retinal and choroidal diseases.

Methods—PUBMED (<http://www.ncbi.nlm.nih.gov/sites/entrez?db=pubmed>) was used for most of the literature search for this article. The criterion for inclusion of an article in the references for this review was that it included materials about both the clinical and the basic properties of choroidal imaging using spectral-domain optical coherence tomography.

Results—Recent reports show successful examination and accurate measurement of choroidal thickness in normal and pathologic states using spectral-domain optical coherence tomography systems. This review focuses on the principles of the new technology that make choroidal imaging using optical coherence tomography possible and on the changes that subsequently have been documented to occur in the choroid in various diseases. Additionally, it outlines future directions in choroidal imaging.

Conclusion—Optical coherence tomography is now proven to be an effective noninvasive tool to evaluate the choroid and to detect choroidal changes in pathologic states. Additionally, choroidal evaluation using optical coherence tomography can be used as a parameter for diagnosis and follow-up.

Keywords

optical coherence tomography; choroid; age-related macular degeneration; central serous chorioretinopathy; diabetic retinopathy

The term choroid is derived from the Greek words for “membrane” and “form.” Histologic investigations of this tissue have been performed since the 17th century. The choroid is a vascularized and pigmented tissue that extends from the ora serrata anteriorly to the optic nerve posteriorly. According to histopathologic examination, it is 0.22 mm thick posteriorly and 0.10 mm to 0.15 mm thick anteriorly.¹

A structurally and functionally normal choroidal vasculature is essential for retinal function: abnormal choroidal blood volume and/or compromised flow can result in photoreceptor dysfunction and death.² Consequently, the choroid plays a vital role in the pathophysiology of many conditions, such as central serous chorioretinopathy (CSC),³ age-related macular degeneration (AMD),⁴ choroidal melanoma,⁵ Vogt–Koyanagi–Harada (VKH),⁶ and others.

A precise clinical understanding of choroidal changes showed proves to be critical for an accurate assessment of many posterior segment diseases. Until recently, the choroid could only be evaluated by indocyanine green (ICG) angiography,^{7,8} laser Doppler flowmetry,⁹ and ultrasound.

Indocyanine green angiography enables visualization of the choroidal vessels and blood flow below the retinal pigment epithelium (RPE) from the posterior pole to the periphery as well as the vortex veins. Indocyanine green angiography may reveal greater detail of a choroidal neovascularization and detect choroidal polyps, versus fluorescein angiogram (FA). The specific properties of ICG with longer wavelength fluorescence and limited diffusion within the choriocapillaris enhance the visualization of structures beneath blood, exudates, or RPE detachments in greater detail.^{10–13}

Laser Doppler flowmetry is a technique that allows noninvasive measurement of hemodynamic parameters of the optic nerve head (ONH), iris, and subfoveal choroidal circulation. Using laser Doppler flowmetry, the mean speed of the erythrocytes in the sampling volume and the number of moving erythrocytes in this volume can be determined. Several studies with laser Doppler flowmetry showed a decrease in volume in the choroidal circulation in various diseases like diabetic retinopathy, AMD, and retinitis pigmentosa.^{14–16}

Ultrasound also plays a role in the diagnosis and management of a variety of vitreoretinal pathologies, especially in the presence of opaque media. Additionally, it can detect and characterize tumors and other thickenings in the choroid and retina. However, the image resolution is low, which makes the detection of small changes in the choroid difficult.¹⁷

Although these techniques are useful for determining vessel abnormalities or changes in the choroidal blood flow, they do not provide three-dimensional anatomical information about the RPE or the choroidal layers. The development of optical coherence tomography (OCT) makes it possible to have high-quality, cross-sectional images of the macula or ONH, analogous to ultrasonography but with greater resolution. However, adequate morphologic examination of the choroid using OCT has not been possible until recently, owing to its posterior location and the presence of pigmented cells in the RPE that attenuate the incident light. Recent reports demonstrated successful examination and measurement of choroidal thickness in normal and pathologic states using spectral-domain optical coherence tomography (SDOCT) instruments.^{4,18–22}

This review focuses on choroidal imaging using SDOCT instruments. It will first review the principles of the new technology that make choroidal imaging using SDOCT possible. Afterward, it will discuss the interpretation of normal choroid OCT images. Then, it will describe the changes occurring in the choroid in different diseases and the usefulness of SDOCT in monitoring treatment response. Additionally, it outlines future directions in choroidal imaging.

Improved Optical Coherence Tomography Technology

Optical coherence tomography uses light waves to obtain a reflectivity versus depth profile of the tissue under investigation.²³ Light from a broadband light source is divided into a reference beam traveling a known path and a sample beam that is directed onto the subject's

retina. Light backscattered by retinal structures interferes with light from the reference beam that has traveled a known path delay. This interference is used to measure the light echoes versus delay or depth. Earlier OCT systems, such as the Stratus OCT (Carl Zeiss Meditec, Inc, Dublin, CA), use time-domain detection, in which the reference mirror position and delay are mechanically scanned to sequentially measure echoes from different depths and produce axial scans (A-scans). Scan rates of 400 A-scans per second with an axial resolution of 8 μm to 10 μm in the eye are achieved with the Stratus OCT.²⁴

More recently, spectral domain, a type of Fourier domain detection, which uses an interferometer with a high-speed spectrometer to measure light echoes from all time delays simultaneously, has become commercially available in multiple OCT platforms. In SDOCT, the reference mirror does not require mechanical scanning and light echoes are detected simultaneously by measuring and Fourier transforming the interference spectrum. Increased sensitivity enables dramatic improvements in image acquisition speed and signal-to-noise ratio.^{25,26} Commercially available SDOCT devices, coupled with improvements in light sources, achieve axial scanning speeds of 20,000 to 52,000 A-scans per second with an axial resolution of 5 μm to 7 μm in the eye.

The choroid cannot usually be well visualized using time-domain OCT. The RPE is highly scattering and attenuates the OCT signal from the choroid. Because of the relatively low signal-to-noise ratio of time-domain OCT compared with SDOCT, there is less signal and image information detected from the deeper layers of the choroid. The pixel density of time-domain OCT, which is limited by the number of axial scans in the OCT image, also makes visualization of fine detail difficult in any part of the retina, including the choroid.

The outer limit of the choroid and the sclera cannot usually be reliably identified using standard SDOCT. In SDOCT, depth information is encoded as different frequencies of the interference spectrum. With increasing depth into tissue, echoes occur further from the point of detection, which is known to be the “zero delay line.” These echoes are more difficult to discern from one another by the spectrometer because they have a higher frequency modulation than echoes found closer to the zero delay line. Two ways to overcome this is to increase the sensitivity of the spectrometer to higher frequency modulation and to increase pixel number in the line scan camera. The sensitivity to frequency modulation of a spectrometer does not have an impact on the resolution of the SDOCT imaging system because axial resolution is determined by the bandwidth of the light source and not by the sensitivity in depth.

Therefore, retinal structures that are closer to the zero delay line have higher signals than structures that are farther from zero delay line. By convention, commercial SDOCT machines operate with the inner retina closest to the zero delay line to maximize the sensitivity from the retina and vitreoretinal interface. In this way, the retina image is improved but it leaves the outer choroid farther from the zero delay line with subsequent diminished signal. Imaging the choroid using SDOCT requires specific imaging protocols that have been described recently. The most important technique to visualize the choroid uses the multiple scans obtained from the same retinal location that are subsequently averaged together by the OCT software. Between scans, the signal should remain constant while any noise is variable. When the subsequent images are averaged, the software reduces the “speckle,” which enhances the continuity and sharper the tissue features. This technique also results in images with improved continuity of retinal features (Figure 1). Averaging typically increases signal-to-noise ratio in proportion to the square root of the number of images averaged. Most commercially available SDOCT devices have image averaging as an option. The different commercial available softwares average 8 to 100 images. At present, there is no consensus about the optimal number of images that should be averaged to

adequately visualize the choroid. In addition to image averaging, several devices have mechanical eye tracking as a feature to ensure that all the images to be averaged are taken from the same retinal location. This also increases signaling by reducing the motion artifact.

Spectral domain detection cannot distinguish between positive and negative echo delays because the interference spectra are identical for an echo at a given positive or negative delay. Therefore, if a retinal structure crosses the zero delay line, it will appear reflected about the zero delay position, as a mirror-like image with reversed depth sensitivity.²⁷ This characteristic can be used to enhance choroidal imaging. If the scan operator advances the sample arm (patient interface) toward the patient so that the mirror image becomes fully apparent, this mirror image can be obtained as the main image. Because the mirror image is inverted about the zero delay line, the information from the choroid–sclera junction in the mirror image is maximized about the vitreous and inner retina. In other words, the decreased detection sensitivity in the choroid is minimized because the choroid–sclera interface is closer to the zero delay line in the mirror image (Figure 2). This technique was first reported by Spaide et al²⁷ as enhanced depth imaging (EDI). EDI is an acquisition software option on several commercial available devices. The EDI software automatically captures the cross-sectional image with the choroid close to the zero delay line to maximize the sensitivity on the outer limit of the choroid.

Normal Choroidal Imaging

Normal choroidal thickness has been described by Margolis et al¹⁹ using the Spectralis (Heidelberg Engineering, Heidelberg, Germany) (Figure 3) and by Manjunath et al²² using the Cirrus HD-OCT (Carl Zeiss Meditec, Inc) (Figure 4). The choroidal thickness was measured manually perpendicularly from the outer edge of the hyperreflective RPE to the inner sclera (choroid–sclera junction) using the OCT software (Figure 4). Both groups report that the choroid is thickest subfoveally and thins nasally more than temporally. The reported subfoveal choroidal thickness was $287 \pm 76 \mu\text{m}$ (mean \pm SD) on the Spectralis with a sample size of 30 patients (54 eyes) and $272 \pm 81 \mu\text{m}$ on the Cirrus device with a sample size of 34 subjects (34 eyes). Both groups also found a negative correlation between choroidal thicknesses and age.^{19,22}

A recent study demonstrated a high reliability and reproducibility for the choroidal thickness measurements in normal subjects. In this investigation, 6 independent examiners measured manually the subfoveal choroidal thickness on horizontal B-scan images. The reliability was evaluated by intraclass correlation coefficient, and the intervisit reproducibility was assessed by examining 10 volunteers, 4 months later. This study showed an interexaminer correlation of 0.970 (95% confidence interval [CI], 0.948–0.985) and an intervisit correlation of 0.893 (95% CI, 0.864–0.916).²⁸

The ability to reliably image the choroid with different SDOCT instruments makes this an emerging area of study. Consequently, it is important to validate the reproducibility of the choroidal measurements by different instruments to understand how precise and comparable the measurements are. A recent investigation analyzed the reproducibility between choroidal thickness measurements of images acquired with Cirrus HD-OCT (Carl Zeiss Meditec, Inc), Spectralis (Heidelberg Engineering), and Optovue RTVue (Optovue, Inc, Fremont, CA).¹⁸ Choroidal thickness of normal eyes was manually measured in five areas. The measurements from any pair of three instruments (Cirrus vs. Spectralis, Cirrus vs. RTVue, Spectralis vs. RTVue) were strongly correlated. The intraclass correlation coefficient between all 2 system pairs of the 3 systems was >0.9 ($P < 0.0001$).

In addition, to evaluate the choroidal thickness, it is important to analyze the choroidal morphology, which may be altered in pathologic conditions. A recent study characterized

the choroidal morphology in 42 eyes of 42 normal subjects. All subjects on this study had a bowl-shaped choroid–sclera junction; 98.8% of subjects had an even distribution of choroidal vessels in the nasal–temporal axis. The thickness of the large vessel layer at the fovea corresponded to 80% of the total subfoveal choroidal thickness.²⁹

Choroidal Imaging and Diseases

Table 1 summarizes the chorioretinal diseases that affect the choroidal thickness.

Central Serous Chorioretinopathy

Central serous chorioretinopathy is a disease characterized by an exudative detachment of the neurosensory retina. Studies using ICG angiography revealed diffuse hyperpermeability of the choroidal vessels much larger than the active RPE leaks seen in the FA, suggesting generalized choroidal vascular disturbance.³ On OCT, CSC appears as an elevation of the full-thickness neurosensory retina from the highly reflective RPE–choriocapillaris complex separated by an optically empty zone. Retinal pigment epithelial detachments may also be detected usually within the areas corresponding to leakage in the FA. In addition, recent separated investigations using 3 different SDOCT devices,^{21,30,31} demonstrated significantly increased choroidal thickness in patients with acute CSC. Using Spectralis (Heidelberg Engineering), the mean (\pm SD) choroidal thickness in 28 eyes of 19 patients with CSC was 505 (\pm 124) μ m (range, 439 μ m–573 μ m), which was 214 μ m (85%) greater than the mean choroidal thickness of age-matched normal eyes ($P = 0.001$) (Figure 5). Additionally, 2 studies evaluated both eyes of patients with unilateral CSC and observed that increased choroidal thickness was present in both eyes: the affected eyes ($445.58 \pm 100.25 \mu$ m) and in the unaffected fellow eyes ($378.35 \pm 117.44 \mu$ m) compared with normal eyes ($266.80 \pm 55.45 \mu$ m).^{32,33} Although the pathophysiology of CSC remains elusive, these findings provide additional evidence that CSC may be caused by increased hydrostatic pressure in the choroid.^{21,31}

In most eyes with CSC, the neurosensory retinal detachment resolves spontaneously within 3 months of duration. However, some patients present with persistent detachment and symptoms after 4 months, suggesting a chronic form of CSC. In these patients, treatment with laser photocoagulation or photodynamic therapy (PDT) is considered. Maruko et al³⁴ measured the subfoveal choroidal thickness before and after the treatment in 20 eyes of 20 patients with chronic CSC, using SDOCT. In this study, 8 eyes were treated with PDT and 12 eyes with laser photocoagulation. A significant decrease in the choroidal thickness after 4 weeks was found in all eyes treated with PDT ($389 \pm 106 \mu$ m at baseline vs. $330 \pm 103 \mu$ m after 4 weeks; $P < 0.001$). Patients treated with laser photocoagulation did not demonstrate a reduction in the choroidal thickness ($345 \pm 127 \mu$ m at baseline vs. $340 \pm 124 \mu$ m after 4 weeks; $P = 0.2$). A similar study examining choroidal thickness in 16 patients (16 eyes) with CSC before and after PDT showed a decrease in the subfoveal choroidal thickness after the treatment (from 421 μ m [95% CI, 352–489 μ m] to 346 μ m [95% CI, 278–414]; $P = 0.0001$).³⁵ Another investigation also showed that half-dose PDT resulted in thinner subfoveal choroidal thickness (80 μ m, 20%) 1 month after treatment, decreased the choroidal vascular hyperpermeability, and maintained the remission for 1 year.³⁶ These findings may suggest that PDT reduces the choroidal vascular hyperpermeability observed in CSC.^{34,36}

The choroidal thickness may be used as an additional parameter to assist in the differentiation of CSC from other causes of serous retinal detachment. In addition, the choroidal thickness may indicate the activity of the disease on the follow-up after treatment with PDT.

Age-Related Macular Degeneration

Age-related macular degeneration is the leading cause of blindness in both developed and developing nations in people older than 60 years.³⁷ Optical coherence tomography, together with clinical biomicroscopy, color fundus photography, FA, autofluorescence imaging, and ICG angiography, is used in the evaluation of patients with AMD. Macular thickness maps generated by the OCT have been shown to be useful in monitoring the progression and treatment response to disease states, such as neovascular AMD after antiangiogenic treatment.³⁸ Choroidal structure is of particular interest in AMD because abnormalities of the choroidal circulation have been hypothesized to contribute to the development of AMD. However, little is currently known about the choroid-related changes using SDOCT in this disease.

Spaide⁴ described a distinct entity, termed age-related choroidal atrophy, which has some overlap with dry AMD. He described 28 eyes of 17 patients with a mean age of 80.6 ± 7.3 years, with mean choroidal thickness less than $125 \mu\text{m}$. The mean subfoveal choroidal thickness was $69.8 \mu\text{m}$, and 35.7% (10 of 28) of the eyes presented with late-stage AMD (Figure 6). It suggests that choroidal thickness decreases with increasing age and the choroidal circulation might play a role in the pathophysiology of AMD.⁴

Another study compared subfoveal choroidal thickness in eyes with neovascular AMD (21 eyes of 21 patients) with that of eyes with polypoidal choroidal vasculopathy (PCV) (23 eyes of 23 patients). This study demonstrated that eyes with PCV have a thicker subfoveal choroid ($293 \pm 72.3 \mu\text{m}$) when compared with eyes featuring typical neovascular AMD ($245 \pm 73.1 \mu\text{m}$), $P = 0.032$ ³⁹ (Figure 6). Additionally, it was found that eyes with a subfoveal choroidal thickness of $> 300 \mu\text{m}$ are more than 5 times more likely to have PCV. Similar results were also observed in another study that compared the choroidal thickness among eyes with neovascular AMD, PCV, and CSC. It was demonstrated that the choroid was thicker in eyes with PCV and CSC than in normal subjects or in those with neovascular AMD.³¹ The thicker choroid could be partially attributed to the dilation of middle and large choroidal vessels or an increase in the choroidal vascular permeability that is observed by ICG.³⁹

Both PCV and neovascular AMD feature abnormal vascular lesions arising from the choroidal vessels, which lead to recurrent serous exudation and hemorrhages. Some studies suggest that PCV lesions respond better to focal treatment with laser or PDT as compared with lesions from neovascular AMD. Sometimes it is difficult to differentiate both diseases. Therefore, the choroidal thickness may play a role in the differentiation of these diseases because the choroid is thinner in eyes with neovascular AMD and the choroid is thicker in eyes with PCV.

Diabetic Retinopathy

Clinical and experimental findings suggest that choroidal vasculopathy in diabetes may play a role in the pathogenesis of diabetic retinopathy. Various choroidal abnormalities, including obstruction of the choriocapillaris, vascular degeneration, choroidal aneurysms, and choroidal neovascularization, have been reported in histopathologic studies of diabetic eye.^{40,41} Esmaeelpour et al⁴² reported central choroid thinning in all Type 2 diabetic eyes regardless of disease stage. Sixty-three eyes were studied, and the choroidal thickness mapping of all diabetic patients demonstrated central and inferior thinning compared with healthy eyes (unpaired *t*-test; $P < 0.001$). Subfoveal choroidal thickness for healthy eyes was $327 \pm 74 \mu\text{m}$, which was found to be significantly thicker than all diabetic eyes: eyes with microaneurysm, $208 \pm 49 \mu\text{m}$; eyes with exudates, $205 \pm 54 \mu\text{m}$; and eyes with clinically significant macular edema $211 \pm 76 \mu\text{m}$ (ANOVA, $P < 0.001$; Tukey, $P < 0.001$).⁴² It can be

speculated that the thinner choroid indicates an overall reduction of choroidal blood flow in diabetic patients, as was previously demonstrated with laser Doppler flowmetry and ICG angiography.^{9,43,44} Therefore, it is likely that the decreased choroidal thickness may be related to retinal tissue hypoxia because the choroid is the major source of nutrition for the RPE and outer retinal layers.

High Myopia

Myopia is the result of a mismatch between the optical power and the length of the eye, with the latter being too long. In high myopia, there is an increased risk of visual impairment and blindness due to ensuing pathologies, such as retinal detachments and choroidal neovascularization. The excessive elongation affects not only the retina but also the choroid and Bruch membrane. Histologic studies demonstrated choroidal thinning in eyes with high myopia due to significant thinning of the choriocapillaris and focal lack of vessels. Fujiwara et al²⁰ studied the subfoveal choroidal thickness in 55 eyes of 31 patients with high myopia (> 6 diopters) using SDOCT. The mean age was 59.7 ± 17.6 years and the mean refractive error was -11.9 ± 3.7 diopters. The authors demonstrated a very thin choroid (93.2 ± 62.5 μm) in highly myopic eyes (Figure 7), and the choroidal thickness was negative correlated with age ($P = 0.006$), refractive error ($P < 0.001$), and history of choroidal neovascularization ($P = 0.013$).²⁰ Additionally, this study suggested that subfoveal choroidal thickness decreases by 12.7 μm for each decade of life and by 8.7 μm for each diopter of increasing myopia. Furthermore, the choroidal thickness may be a predictive factor for visual acuity in highly myopic patients because the choroid is responsible for the oxygen and nutrient supply of the outer retina.

Uveitis

The SDOCT is now proven to be an effective noninvasive investigation tool for detecting pathologic features in uveitis and is gaining more popularity as an ancillary examination in patients with posterior segment manifestations of uveitis.^{45,46}

Vogt–Koyanagi–Harada disease is a bilateral granulomatous panuveitis associated with autoimmunity against melanocytes. The acute uveitic stage of VKH is characterized by bilateral anterior and/or posterior segment involvement with exudative retinal detachment.⁴⁷ Indocyanine green shows patchy filling delays with hypofluorescent spots, and in addition, B-scan ultrasound shows anatomical alterations.⁴⁸ Maruko et al⁶ studied the choroidal thickness of 16 patients (32 eyes) with active VKH disease before and after corticosteroid treatment. All eyes had markedly thickened choroid (805 ± 173 μm vs. 287 ± 76 μm of normal eyes) before the treatment, possibly related not only to inflammatory infiltration but also to increased exudation. Additionally, a reduction in the choroidal thickness was documented after 2 weeks of corticosteroid treatment (baseline: 805 ± 173 μm ; 2 weeks of follow-up: 341 ± 70 μm , $P < 0.001$).⁶ Evaluating the choroidal thickness has potential importance for assessing treatment efficacy and recurrence in VKH disease. Another study investigated the choroid of six VKH patients in acute and convalescent stages. A loss of focal hyperreflectivity in the inner choroid. The presence of this feature in both acute and convalescent phases suggests that there is a permanent structural change to small choroidal vessels caused by VKH uveitis.⁴⁹ Choroidal imaging using SDOCT may change the treatment strategies used for VKH. In the past, treatment with high dose of corticosteroids was initiated and then tapered off rapidly. If the corticosteroids were tapered too rapidly, the serous detachment returned. It is conceivable that gauging the proper corticosteroid taper can be more safely done by monitoring the choroidal thickness with SDOCT.

Choroidal changes are also described in multifocal choroiditis. Yasuno et al,⁵⁰ using an SDOCT with 1060 nm wavelength studied 1 patient with multifocal choroiditis and showed

localized thinning of the choroid, occlusion of the choroidal vessels, and localized hyperreflectivity that may represent hyperpigmentation of the choroid. Another study investigated three cases with acute lesions of multifocal choroiditis using Spectralis (Heidelberg Engineering). This study reported the findings of acute lesions, which include presence of sub-RPE material, choroidal hyperreflectivity below these lesions, and overlying vitreous cells.⁵¹

Tumors

The SDOCT of the choroid has also been used to examine choroidal tumors. Torres et al⁵ found that features such as the delineation of the borders of the tumor both parallel and perpendicular to the visual axis along with evaluation of the inner choriocapillaris and outer large vessels within the tumor was possible: in around half of eyes examined (10 of 23), the axial thickness of the tumor was able to be identified using SDOCT as compared with ultrasound, which was able to detect the extent of all tumors examined. Another study evaluated 11 eyes with choroidal osteoma. The tumor was hyporeflective in two cases, isoreflective in seven cases, and hyperreflective in two cases. Additionally, it was observed that overlying choroid was compressed by the tumor in 72.7% and the retina exhibited degenerative changes in 45.5% of the cases.⁵² These studies demonstrate that SDOCT allows characterization of the thickness and reflective quality of small (<3 mm thick) choroidal lesions including choroidal nevi and melanomas. Future improvements in image resolution and depth will allow better understanding of the mechanisms of visual loss, tumor growth, and tumor management.^{5,52,53}

Retinal Dystrophies

The SDOCT has been used to investigate a number of structural abnormalities in the retina of subjects with inherited retinal dystrophies, including retinitis pigmentosa.⁵⁴ The choroid has been implicated in the pathophysiology of a number of these dystrophies as well.¹ Furthermore, using scanning Doppler flowmetry, choroidal blood flow has been demonstrated to be diminished in subjects with retinitis pigmentosa when compared with that of normal subjects and that this decrease correlates with cone function¹⁶ (Figures 8 and 9). Using EDI OCT, Yeoh et al⁵⁵ found changes in the structure of the choroid in a subset of a heterogeneous group of subjects with retinal dystrophies. The observed changes include both focal and diffuse choroidal thinning (Figure 8). These changes do not appear to be associated with visual acuity.⁵⁵

Glaucoma

Choroidal imaging as a tool to investigate the vascular theory of glaucoma pathogenesis has evaluated both the macular choroid and the peripapillary choroid. Normal peripapillary choroidal thickness was described by Ho et al.⁵⁶ This investigation of 36 normal subjects imaged with both horizontal and vertical raster scans concluded that the inferior quadrant ($149.90 \pm 50.14 \mu\text{m}$) was significantly thinner than the superior ($229.41 \pm 50.96 \mu\text{m}$), nasal ($227.17 \pm 81.40 \mu\text{m}$), and temporal ($208.84 \pm 55.70 \mu\text{m}$) quadrants ($P < 0.001$).

Maul et al⁵⁷ described a relationship between macular choroidal thickness as measured using EDI OCT and age, axial length, and nerve fiber layer loss. However, when compared with glaucoma suspects ($n = 37$), Maul et al⁵⁷ did not find a significant difference in macular or peripapillary choroidal thickness in glaucomatous eyes ($n = 37$) ($14 \mu\text{m}$ [95% CI, -54 to 26]; $P = 0.5$).

Similarly, Mwanza et al⁵⁸ reported no significant difference in macular choroidal thickness between 38 normal subjects, 20 normal-tension glaucoma patients, and 56 primary open-angle glaucoma patients using EDI OCT. Ehrlich et al⁵⁹ confirmed these results in finding

no difference in peripapillary choroidal thickness between glaucoma suspects ($n = 39$) and patients with primary open-angle glaucoma ($n = 31$) ($P = 0.13$). One consideration when interpreting these data is that both groups studied glaucoma suspects rather than healthy subjects as the control group.

In contrast, Usui et al⁶⁰ found significantly decreased choroidal thickness both in the macula and in the region of the ONH in highly myopic eyes with normal-tension glaucoma as compared with age- and refraction-matched healthy controls (fovea: 166 μm vs. 276 μm , $P < 0.001$; superior ONH: 172 μm vs. 241 μm , $P < 0.05$; superotemporal ONH: 161 μm vs. 244 μm , $P < 0.01$; temporal ONH: 110 μm vs. 161 μm , $P < 0.01$; and inferotemporal ONH: 115 μm vs. 159 μm , $P < 0.05$). Usui et al⁶⁰ used a prototypical swept-source OCT with a scan speed of 50,000 A-scans per second at 1060 nm.

Using EDI OCT, Park et al⁶¹ further investigated peripapillary imaging of glaucomatous eyes. They found in 139 eyes (73 patients) with glaucoma that the anterior surface of the lamina cribrosa was identifiable in 65% of eyes and that pores within the lamina cribrosa were identifiable in 76% of eyes. In 86% of eyes, the short posterior ciliary artery was identified. In 18% of eyes, the subarachnoid space was identified. Given that these structures have been implicated in the pathogenesis of glaucoma, in addition to choroidal imaging, SDOCT may be used in the future to investigate the relationship of these structures with glaucoma in vivo.

Future Directions in Choroidal Imaging

Because of the posterior location of the choroid, OCT imaging is difficult because incident light is attenuated by the RPE and retinal structures. One method to increase the depth of choroidal penetration by OCT is to image with a longer wavelength of incident light to reduce attenuation from scattering.⁶² One such approach has been to use an incident wavelength centered near 1050 nm, which is absorbed minimally by water in the vitreous. Prototype systems with 1050 nm wavelength and axial resolution of 7 μm have demonstrated increased choroidal visualization when compared with standard SDOCT using a wavelength centered ~800 nm.⁶³ Likewise, SDOCT systems using 1050 nm wavelength have demonstrated increased penetration through cataracts and media opacities when compared with systems using 800 nm wavelength.⁶⁴

Another method that may improve imaging the choroid is the swept source optical coherence tomography (SSOCT).^{65–67} The SSOCT uses a tunable frequency swept laser light source to increase signal quality deeper in tissue when compared with SDOCT. The light source of SSOCT is able to sequentially emit various frequencies in time. This means that the interference spectrum is measured by photodetectors rather than by a spectrometer and line scan camera, as is the case in SDOCT. Consequently, decreased sensitivity of a spectrometer to higher frequency modulation is eliminated. Furthermore, k-space is no longer unevenly sampled in SSOCT.^{67–69} This dramatically reduces sensitivity roll-off, thus making image quality deeper in tissues improved.

In SSOCT, the limiting factor in scan acquisition time is the speed at which the light source can sweep the needed frequencies. Because swept laser light sources can do this very rapidly, SSOCT is much faster than SDOCT with axial scan rates of up to 236,000 A-scans per second with 11- μm axial resolution in tissue.^{70,71} This allows for more data acquisition in a given time, making volumetric data sets feasible.⁶⁷

In addition to SSOCT, Doppler OCT is a promising technology in the field of choroidal imaging.^{72–74} Doppler OCT can evaluate blood flow and volume of retinal vasculature.^{75,76} Also, it can highlight vessels where there is blood flow, without quantitatively measuring

flow.⁷⁷ In contrast to FA or ICG angiography, which are 2 dimensional, Doppler OCT is depth resolved, meaning that cross-sectional images can be used to identify in which retinal layers vascular abnormalities occur. This method has been used to evaluate abnormalities in chorioretinal vasculature.⁷⁸ As such, this technology is promising to aid in monitoring chorioretinal diseases, especially neovascular AMD.

Along with modifications in hardware and image acquisition, improvements in software and processing of OCT data will probably be important in the future for evaluation and monitoring of choroidal changes. One such software advance is the use of en-face imaging. This technique allows the clinician to visualize three-dimensional data in a useful way as it shows a particular retinal layer at a given depth projected into an en-face view, which closely corresponds to a fundus image. It is hard to evaluate the health of the choroid using only a limited number of B-scans because the cross-sectional nature makes it such that vessels are transected at odd angles. En-face imaging makes subtle microstructural relationships much more apparent.⁷⁹ This promises to aid in the evaluation of chorioretinal diseases.

Acknowledgments

Supported in part by a Research to Prevent Blindness Unrestricted Grant and Lions Club of Massachusetts Grant to the New England Eye Center/Department of Ophthalmology—Tufts University School of Medicine; National Institutes of Health contracts R01-EY11289-25, R01-EY13178-10, R01-EY013516-07, and R01-EY019029-02; Air Force Office of Scientific Research FA9550-10-1-0551 and FA9550-10-1-0063.

J. S. Duker receives research support from Carl Zeiss Meditech, Inc, Optovue, Inc., and Topcon Medical Systems, Inc. J. G. Fujimoto receives royalties from intellectual property owned by M.I.T. and licensed to Carl Zeiss Meditech, Inc, and has stock options in Optovue, Inc.

References

1. Ryan, SJ. Retina. 4th ed.. Vol. Vol 1. Philadelphia, PA: Elsevier Mosby; 2006. p. 33-34.
2. Cao J, McLeod S, Merges CA, Luty GA. Choriocapillaris degeneration and related pathologic changes in human diabetic eyes. Arch Ophthalmol. 1998; 116:589–597. [PubMed: 9596494]
3. Gemenetzi M, De Salvo G, Lotery AJ. Central serous chorioretinopathy: an update on pathogenesis and treatment. Eye (Lond). 2010; 24:1743–1756. [PubMed: 20930852]
4. Spaide RF. Age-related choroidal atrophy. Am J Ophthalmol. 2009; 147:801–810. [PubMed: 19232561]
5. Torres VL, Brugnoli N, Kaiser PK, Singh AD. Optical coherence tomography enhanced depth imaging of choroidal tumors. Am J Ophthalmol. 2011; 151:586–593. e582. [PubMed: 21257150]
6. Maruko I, Iida T, Sugano Y, Saito M, Sekiryu T. Subfoveal retinal and choroidal thickness after verteporfin photodynamic therapy for polypoidal choroidal vasculopathy. Am J Ophthalmol. 2011; 151:594–603. e1. [PubMed: 21295766]
7. Inoue R, Sawa M, Tsujikawa M, Gomi F. Association between the efficacy of photodynamic therapy and indocyanine green angiography findings for central serous chorioretinopathy. Am J Ophthalmol. 2010; 149:441–446. e441–e442. [PubMed: 20172070]
8. Shiraki K, Moriaki M, Kohno T, et al. Age-related scattered hypofluorescent spots on late-phase indocyanine green angiograms. Int Ophthalmol. 1999; 23:105–109. [PubMed: 11196117]
9. Nagaoka T, Kitaya N, Sugawara R, et al. Alteration of choroidal circulation in the foveal region in patients with type 2 diabetes. Br J Ophthalmol. 2004; 88:1060–1063. [PubMed: 15258025]
10. Rosen RB, Hathaway M, Rogers J, et al. Simultaneous OCT/SLO/ICG imaging. Invest Ophthalmol Vis Sci. 2009; 50:851–860. [PubMed: 18952928]
11. Spaide RF, Yannuzzi LA, Slakter JS, et al. Indocyanine green videoangiography of idiopathic polypoidal choroidal vasculopathy. Retina. 1995; 15:100–110. [PubMed: 7542796]
12. Yannuzzi LA. Indocyanine green angiography: a perspective on use in the clinical setting. Am J Ophthalmol. 2011; 151:745–751. e741. [PubMed: 21501704]

13. Desmettre T, Devoisselle JM, Mordon S. Fluorescence properties and metabolic features of indocyanine green (ICG) as related to angiography. *Surv Ophthalmol.* 2000; 45:15–27. [PubMed: 10946079]
14. Pemp B, Schmetterer L. Ocular blood flow in diabetes and age-related macular degeneration. *Can J Ophthalmol.* 2008; 43:295–301. [PubMed: 18443612]
15. Luty G, Grunwald J, Majji AB, et al. Changes in choriocapillaris and retinal pigment epithelium in age-related macular degeneration. *Mol Vis.* 1999; 5:35. [PubMed: 10562659]
16. Falsini B, Anselmi GM, Marangoni D, et al. Subfoveal choroidal blood flow and central retinal function in retinitis pigmentosa. *Invest Ophthalmol Vis Sci.* 2011; 52:1064–1069. [PubMed: 20861481]
17. Malhotra A, Minja FJ, Crum A, Burrowes D. Ocular anatomy and cross-sectional imaging of the eye. *Semin Ultrasound CT MR.* 2011; 32:2–13. [PubMed: 21277487]
18. Branchini L, Regatieri CV, Flores-Moreno I, Baumann B, Fujimoto JG, Duker JS. Reproducibility of choroidal thickness measurements across three spectral domain optical coherence tomography systems. *Ophthalmology.* 2012; 119:119–123. [PubMed: 21943786]
19. Margolis R, Spaide RF. A pilot study of enhanced depth imaging optical coherence tomography of the choroid in normal eyes. *Am J Ophthalmol.* 2009; 147:811–815. [PubMed: 19232559]
20. Fujiwara T, Imamura Y, Margolis R, et al. Enhanced depth imaging optical coherence tomography of the choroid in highly myopic eyes. *Am J Ophthalmol.* 2009; 148:445–450. [PubMed: 19541286]
21. Imamura Y, Fujiwara T, Margolis R, Spaide RF. Enhanced depth imaging optical coherence tomography of the choroid in central serous chorioretinopathy. *Retina.* 2009; 29:1469–1473. [PubMed: 19898183]
22. Manjunath V, Taha M, Fujimoto JG, Duker JS. Choroidal thickness in normal eyes measured using Cirrus HD optical coherence tomography. *Am J Ophthalmol.* 2010; 150:325–329. e321. [PubMed: 20591395]
23. Huang D, Swanson EA, Lin CP, et al. Optical coherence tomography. *Science.* 1991; 254:1178–1181. [PubMed: 1957169]
24. Sull AC, Vuong LN, Price LL, et al. Comparison of spectral/Fourier domain optical coherence tomography instruments for assessment of normal macular thickness. *Retina.* 2010; 30:235–245. [PubMed: 19952997]
25. de Boer JF, Cense B, Park BH, et al. Improved signal-to-noise ratio in spectral-domain compared with time-domain optical coherence tomography. *Opt Lett.* 2003; 28:2067–2069. [PubMed: 14587817]
26. Leitgeb R, Hitzinger C, Fercher A. Performance of fourier domain vs. time domain optical coherence tomography. *Opt Express.* 2003; 11:889–894. [PubMed: 19461802]
27. Spaide RF, Koizumi H, Pozzoni MC. Enhanced depth imaging spectral-domain optical coherence tomography. *Am J Ophthalmol.* 2008; 146:496–500. [PubMed: 18639219]
28. Ikuno Y, Maruko I, Yasuno Y, Miura M, Sekiryu T, Nishida K, et al. Reproducibility of retinal and choroidal thickness measurements in enhanced depth imaging and high-penetration optical coherence tomography. *Invest Ophthalmol Vis Sci.* 2011; 52:5536–5540. [PubMed: 21508114]
29. Nandakumar N, Branchini L, Regatieri CV, et al. Characterization of choroidal morphology in healthy eyes using spectral domain optical coherence tomograph. *Invest Ophthalmol Vis Sci.* 2011; 52 E-Abstract 285.
30. Manjunath V, Fujimoto JG, Duker JS. Cirrus HD-OCT high definition imaging is another tool available for visualization of the choroid and provides agreement with the finding that the choroidal thickness is increased in central serous chorioretinopathy in comparison to normal eyes. *Retina.* 2010; 30:1320–1321. author reply 1321–1322. [PubMed: 20827146]
31. Kim SW, Oh J, Kwon SS, et al. Comparison of choroidal thickness among patients with healthy eyes, early age-related maculopathy, neovascular age-related macular degeneration, central serous chorioretinopathy, and polypoidal choroidal vasculopathy. *Retina.* 2011; 31:1904–1911. [PubMed: 21878855]
32. Kim YT, Kang SW, Bai KH. Choroidal thickness in both eyes of patients with unilaterally active central serous chorioretinopathy. *Eye (Lond).* 2011; 25:1635–1640. [PubMed: 22020172]

33. Maruko I, Iida T, Sugano Y, et al. Subfoveal choroidal thickness in fellow eyes of patients with central serous chorioretinopathy. *Retina*. 2011; 31:1603–1608. [PubMed: 21487334]
34. Maruko I, Iida T, Sugano Y, et al. Subfoveal choroidal thickness after treatment of central serous chorioretinopathy. *Ophthalmology*. 2010; 117:1792–1799. [PubMed: 20472289]
35. Pryds A, Larsen M. Choroidal thickness following extrafoveal photodynamic treatment with verteporfin in patients with central serous chorioretinopathy. *Acta Ophthalmol*. 2011 Epub ahead of print.
36. Maruko I, Iida T, Sugano Y, et al. One-year choroidal thickness results after photodynamic therapy for central serous chorioretinopathy. *Retina*. 2011; 31:1921–1927. [PubMed: 21878850]
37. Klein R, Klein BE, Linton KL. Prevalence of age-related maculopathy. The Beaver Dam Eye Study. *Ophthalmology*. 1992; 99:933–943. [PubMed: 1630784]
38. Fung AE, Lalwani GA, Rosenfeld PJ, et al. An optical coherence tomography-guided, variable dosing regimen with intravitreal ranibizumab (Lucentis) for neovascular age-related macular degeneration. *Am J Ophthalmol*. 2007; 143:566–583. [PubMed: 17386270]
39. Koizumi H, Yamagishi T, Yamazaki T, Kawasaki R, Kinoshita S. Subfoveal choroidal thickness in typical age-related macular degeneration and polypoidal choroidal vasculopathy. *Graefes Arch Clin Exp Ophthalmol*. 2011; 249:1123–1128. [PubMed: 21274555]
40. Hidayat AA, Fine BS. Diabetic choroidopathy. Light and electron microscopic observations of seven cases. *Ophthalmology*. 1985; 92:512–522. [PubMed: 2582331]
41. Weinberger D, Kramer M, Priel E, et al. Indocyanine green angiographic findings in nonproliferative diabetic retinopathy. *Am J Ophthalmol*. 1998; 126:238–247. [PubMed: 9727518]
42. Esmaeelpour M, Povazay B, Hermann B, Hofer B, Kojic V, Hale SL, et al. Mapping choroidal and retinal thickness variation in type 2 diabetes using three-dimensional 1060-nm optical coherence tomography. *Invest Ophthalmol Vis Sci*. 2011; 52:5311–5316. [PubMed: 21508108]
43. Schocket LS, Brucker AJ, Niknam RM, et al. Foveolar choroidal hemodynamics in proliferative diabetic retinopathy. *Int Ophthalmol*. 2004; 25:89–94. [PubMed: 15290887]
44. Shiragami C, Shiraga F, Matsuo T, et al. Risk factors for diabetic choroidopathy in patients with diabetic retinopathy. *Graefes Arch Clin Exp Ophthalmol*. 2002; 240:436–442. [PubMed: 12107509]
45. Gupta V, Gupta A, Gupta P, Sharma A. Spectral-domain cirrus optical coherence tomography of choroidal striations seen in the acute stage of Vogt-Koyanagi-Harada disease. *Am J Ophthalmol*. 2009; 147:148–153. e142. [PubMed: 18834577]
46. Diniz B, Regatieri C, Andrade R, Maia A. Evaluation of spectral domain and time domain optical coherence tomography findings in toxoplasmic retinochoroiditis. *Clin Ophthalmol*. 2011; 5:645–650. [PubMed: 21629569]
47. Bordaberry MF. Vogt-Koyanagi-Harada disease: diagnosis and treatments update. *Curr Opin Ophthalmol*. 2010; 21:430–435. [PubMed: 20829689]
48. Herbot CP, Mantovani A, Bouchenaki N. Indocyanine green angiography in Vogt-Koyanagi-Harada disease: angiographic signs and utility in patient follow-up. *Int Ophthalmol*. 2007; 27:173–182. [PubMed: 17457515]
49. Fong AH, Li KK, Wong D. Choroidal evaluation using enhanced depth imaging spectral-domain optical coherence tomography in Vogt-Koyanagi-Harada disease. *Retina*. 2011; 31:502–509. [PubMed: 21336069]
50. Yasuno Y, Okamoto F, Kawana K, et al. Investigation of multifocal choroiditis with panuveitis by three-dimensional high-penetration optical coherence tomography. *J Biophotonics*. 2009; 2:435–441. [PubMed: 19575418]
51. Vance SK, Khan S, Klancnik JM, Freund KB. Characteristic spectral-domain optical coherence tomography findings of multifocal choroiditis. *Retina*. 2011; 31:717–723. [PubMed: 21386760]
52. Freton A, Finger PT. Spectral domain-optical coherence tomography analysis of choroidal osteoma. *Br J Ophthalmol*. 2012; 96:224–228. [PubMed: 21527415]
53. Say EA, Shah SU, Ferenczy S, Shields CL. Optical coherence tomography of retinal and choroidal tumors. *J Ophthalmol*. 2010; 2011 385058.

54. Witkin AJ, Ko TH, Fujimoto JG, et al. Ultra-high resolution optical coherence tomography assessment of photoreceptors in retinitis pigmentosa and related diseases. *Am J Ophthalmol.* 2006; 142:945–952. [PubMed: 17157580]
55. Yeoh J, Rahman W, Chen F, et al. Choroidal imaging in inherited retinal disease using the technique of enhanced depth imaging optical coherence tomography. *Graefes Arch Clin Exp Ophthalmol.* 2010; 248:1719–1728. [PubMed: 20640437]
56. Ho J, Branchini L, Regatieri C, et al. Analysis of normal peripapillary choroidal thickness via spectral domain optical coherence tomography. *Ophthalmology.* 2011; 118:2001–2007. [PubMed: 21703691]
57. Maul EA, Friedman DS, Chang DS, et al. Choroidal thickness measured by spectral domain optical coherence tomography: factors affecting thickness in glaucoma patients. *Ophthalmology.* 2011; 118:1571–1579. [PubMed: 21492939]
58. Mwanza JC, Hochberg JT, Banitt MR, et al. Lack of association between glaucoma and macular choroidal thickness measured with enhanced depth-imaging optical coherence tomography. *Invest Ophthalmol Vis Sci.* 2011; 52:3430–3435. [PubMed: 21357398]
59. Ehrlich JR, Peterson J, Parlitsis G, et al. Peripapillary choroidal thickness in glaucoma measured with optical coherence tomography. *Exp Eye Res.* 2011; 92:189–194. [PubMed: 21232535]
60. Usui S, Ikuno Y, Miki A, et al. Evaluation of the choroidal thickness using high-penetration optical coherence tomography with long wavelength in highly myopic normal-tension glaucoma. *Am J Ophthalmol.* 2011 Epub ahead of print.
61. Park SC, De Moraes CG, Teng CC, Tello C, Liebmann JM, Ritch R. Enhanced depth imaging optical coherence tomography of deep optic nerve complex structures in glaucoma. *Ophthalmology.* 2012; 119:3–9. [PubMed: 21978593]
62. Unterhuber A, Povazay B, Hermann B, et al. In vivo retinal optical coherence tomography at 1040 nm—enhanced penetration into the choroid. *Opt Express.* 2005; 13:3252–3258. [PubMed: 19495226]
63. Povazay B, Bizheva K, Hermann B, et al. Enhanced visualization of choroidal vessels using ultrahigh resolution ophthalmic OCT at 1050 nm. *Opt Express.* 2003; 11:1980–1986. [PubMed: 19466083]
64. Povazay B, Hermann B, Unterhuber A, et al. Three-dimensional optical coherence tomography at 1050 nm versus 800 nm in retinal pathologies: enhanced performance and choroidal penetration in cataract patients. *J Biomed Opt.* 2007; 12 041211.
65. Chinn SR, Swanson EA, Fujimoto JG. Optical coherence tomography using a frequency-tunable optical source. *Opt Lett.* 1997; 22:340–342. [PubMed: 18183195]
66. de Boer JF, Milner TE, van Gemert MJ, Nelson JS. Two-dimensional birefringence imaging in biological tissue by polarization-sensitive optical coherence tomography. *Opt Lett.* 1997; 22:934–936. [PubMed: 18185711]
67. Drexler W, Fujimoto JG. State-of-the-art retinal optical coherence tomography. *Prog Retin Eye Res.* 2008; 27:45–88. [PubMed: 18036865]
68. Choma MA, Yang C, Izatt JA. Instantaneous quadrature low-coherence interferometry with 3×3 fiber-optic couplers. *Opt Lett.* 2003; 28:2162–2164. [PubMed: 14649928]
69. Choma MA, Hsu K, Izatt JA. Swept source optical coherence tomography using an all-fiber 1300-nm ring laser source. *J Biomed Opt.* 2005; 10 44009.
70. Srinivasan VJ, Huber R, Gorczynska I, et al. High-speed, high-resolution optical coherence tomography retinal imaging with a frequency-swept laser at 850 nm. *Opt Lett.* 2007; 32:361–363. [PubMed: 17356653]
71. Huber R, Adler DC, Srinivasan VJ, Fujimoto JG. Fourier domain mode locking at 1050 nm for ultra-high-speed optical coherence tomography of the human retina at 236,000 axial scans per second. *Opt Lett.* 2007; 32:2049–2051. [PubMed: 17632639]
72. Izatt JA, Kulkarni MD, Yazdanfar S, et al. In vivo bidirectional color Doppler flow imaging of picoliter blood volumes using optical coherence tomography. *Opt Lett.* 1997; 22:1439–1441. [PubMed: 18188263]

73. Leitgeb R, Schmetterer L, Drexler W, et al. Real-time assessment of retinal blood flow with ultrafast acquisition by color Doppler Fourier domain optical coherence tomography. *Opt Express*. 2003; 11:3116–3121. [PubMed: 19471434]
74. White B, Pierce M, Nassif N, et al. In vivo dynamic human retinal blood flow imaging using ultra-high-speed spectral domain optical coherence tomography. *Opt Express*. 2003; 11:3490–3497. [PubMed: 19471483]
75. Wang Y, Lu A, Gil-Flamer J, et al. Measurement of total blood flow in the normal human retina using Doppler Fourier-domain optical coherence tomography. *Br J Ophthalmol*. 2009; 93:634–637. [PubMed: 19168468]
76. Leitgeb RA, Schmetterer L, Hitzenberger CK, et al. Real-time measurement of in vitro flow by Fourier-domain color Doppler optical coherence tomography. *Opt Lett*. 2004; 29:171–173. [PubMed: 14744000]
77. Makita S, Hong Y, Yamanari M, et al. Optical coherence angiography. *Opt Express*. 2006; 14:7821–7840. [PubMed: 19529151]
78. Miura M, Makita S, Iwasaki T, Yasuno Y. Three-dimensional visualization of ocular vascular pathology by optical coherence angiography in vivo. *Invest Ophthalmol Vis Sci*. 2011 Epub ahead of print.
79. Srinivasan VJ, Adler DC, Chen Y, et al. Ultrahigh-speed optical coherence tomography for three-dimensional and en face imaging of the retina and optic nerve head. *Invest Ophthalmol Vis Sci*. 2008; 49:5103–5110. [PubMed: 18658089]

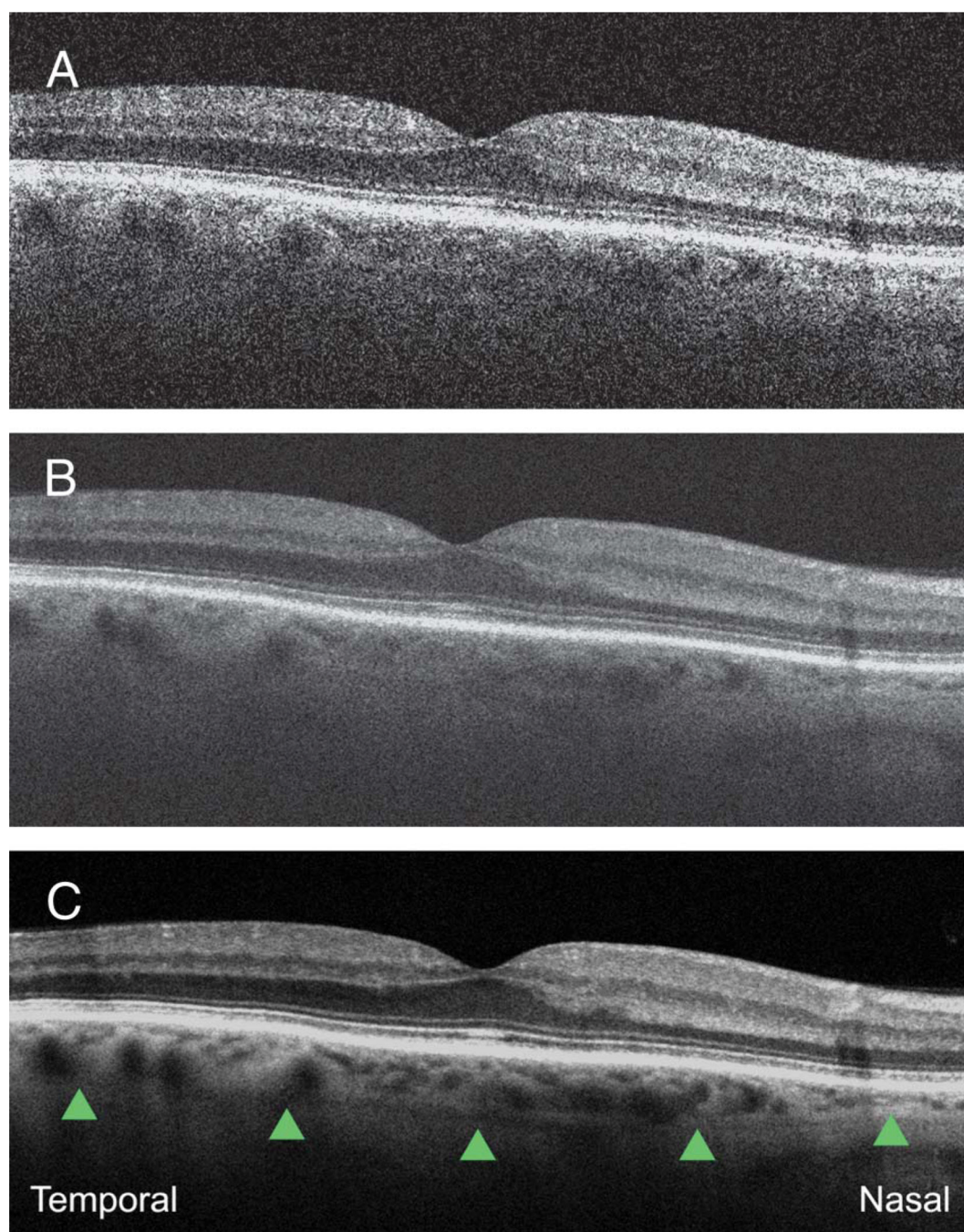


Fig. 1. Optical coherence tomography image demonstrating image averaging using Cirrus HD-OCT (Carl Zeiss Meditec, Inc). **A.** Image is a single B-scan. Note the low signal and indistinct border of the choroid and sclera. **B.** Image is 5 B-scans averaged together. Note the increase in signal from the choroid. **C.** Image is 20 B-scans averaged together. Note the further improvement in signal from image **B** and the distinct delineation of the choroid–sclera junction (green arrowheads).

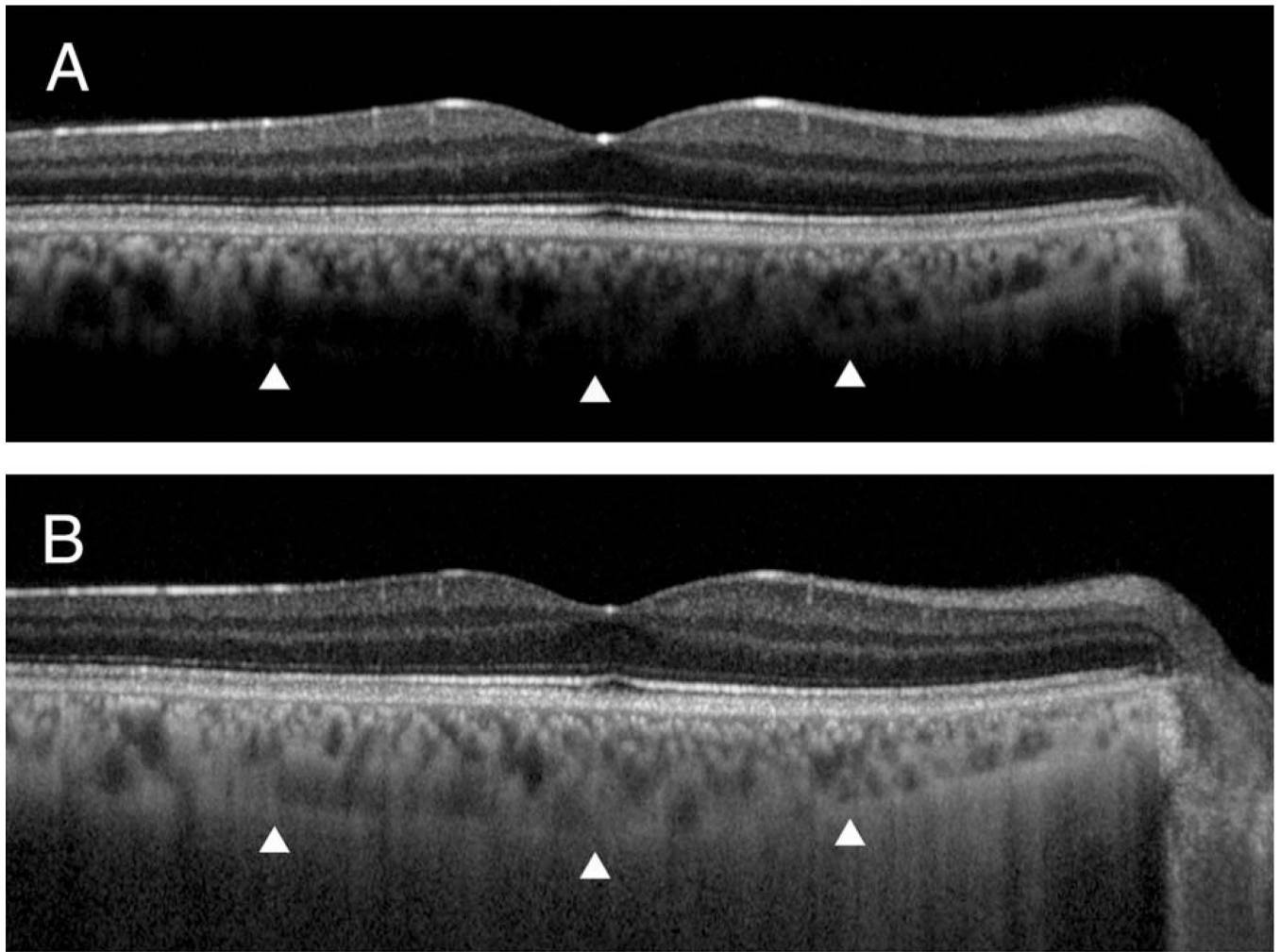


Fig. 2. Optical coherence tomography image demonstrating enhanced depth imaging on Spectralis (Heidelberg Engineering). **A.** Image was acquired with the inner retina adjacent to the zero delay. Note that the choroid-sclera junction is not distinct (white arrowheads) and there is low signal from the choroid but high signal from the inner retina. **B.** Image was acquired with the choroid adjacent to the zero delay by advancing the instrument toward the patient. Note that the choroid-sclera junction is distinct and that there is reduced signal from the inner retina but increased signal from the choroid.

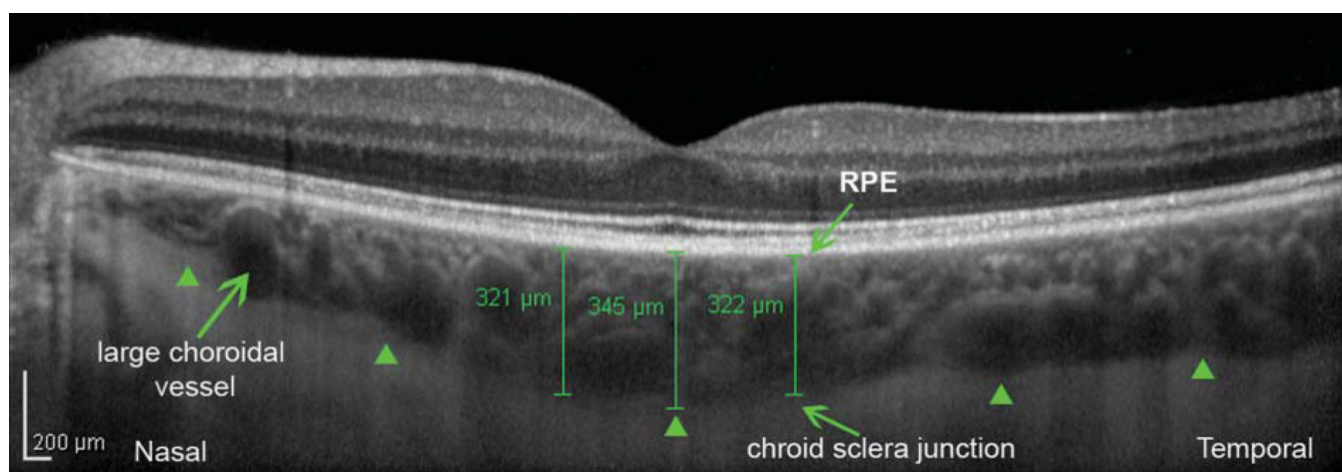


Fig. 3. Optical coherence tomography image of the normal choroid taken on Spectralis with EDI and over sampling. Choroidal thickness was measured in the fovea and at 500- μm intervals, nasal and temporal to the fovea with the measurements expressed in micrometer (green lines). Note the choroid-sclera junction (green arrowheads). Note that it is possible to visualize the choroidal large vessels.

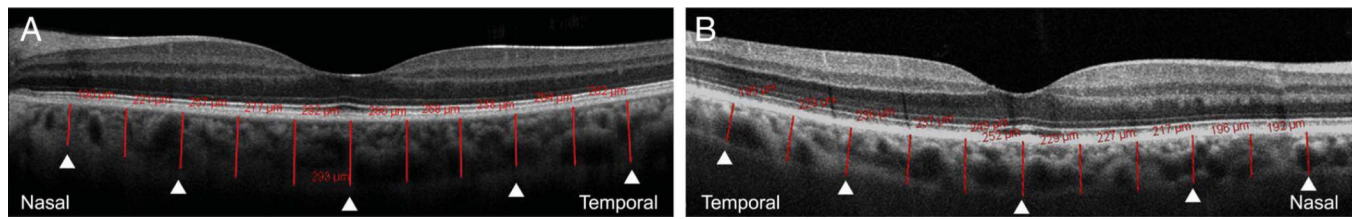


Fig. 4. Optical coherence tomography image of the normal choroid taken on Cirrus HD-OCT with 20 images averaged. **A.** Representative scan from a normal 24-year-old subject. **B.** Representative scan from a normal 76-year-old subject. Note the choroid-sclera junction (white arrowheads). Choroidal thickness was measured in the fovea and at 500- μ m intervals nasal and temporal to the fovea with the measurements expressed in micrometer (red lines). Note that the choroid is thinner in image **B**.

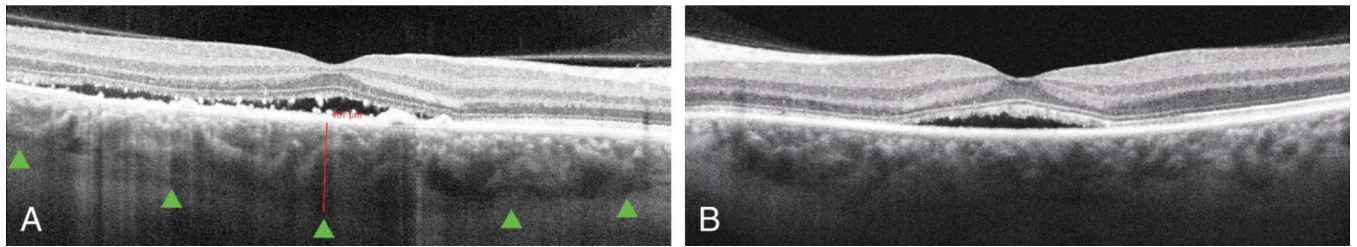


Fig. 5.

Optical coherence tomography image of the choroid of a patient with central serous chorioretinopathy taken on Cirrus HD-OCT with 20 images averaged. **A.** Note that the choroid is thicker in the whole extension. The green arrowheads point the choroid–sclera junction. **B.** Note that it is not possible to visualize the choroid–sclera junction. The choroid may be so thickened as to lose signal penetration and intensity at the increasing depth because of signal roll-off distal to the zero delay line.

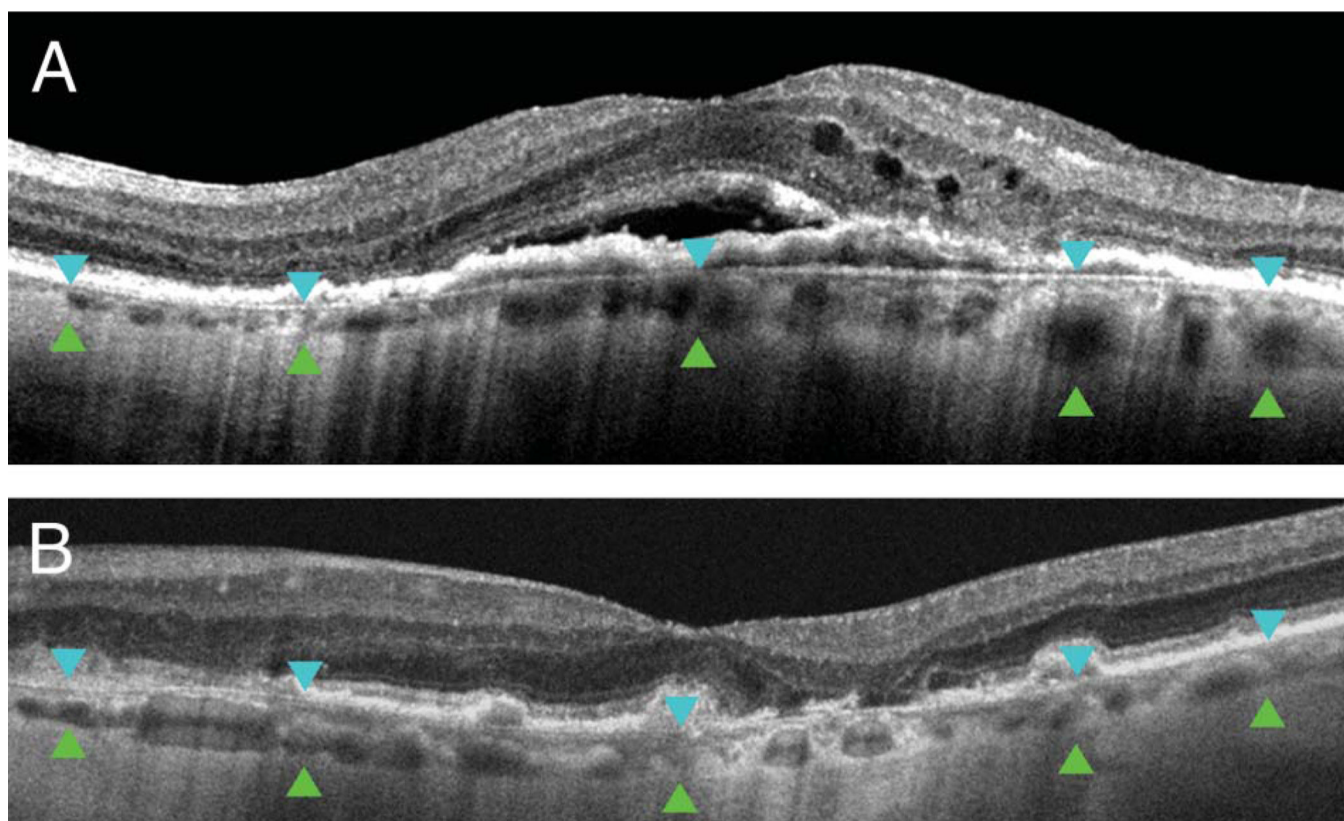


Fig. 6.

A. Optical coherence tomography image of the choroid of a patient with exudative AMD taken on Cirrus HD-OCT with 20 images averaged. Note that the choroid is thin and that it can be visualized beneath choroidal neovascularization. The blue arrowheads point the outer edge of the hyperreflective RPE, and the green arrowheads point the choroid-sclera junction. **B.** Optical coherence tomography image of the choroid of a patient with dry AMD taken on Cirrus HD-OCT with 20 images averaged. Note that the choroid is thin, and in the area of RPE atrophy, it is possible to visualize a hyperreflective area on the choroid.

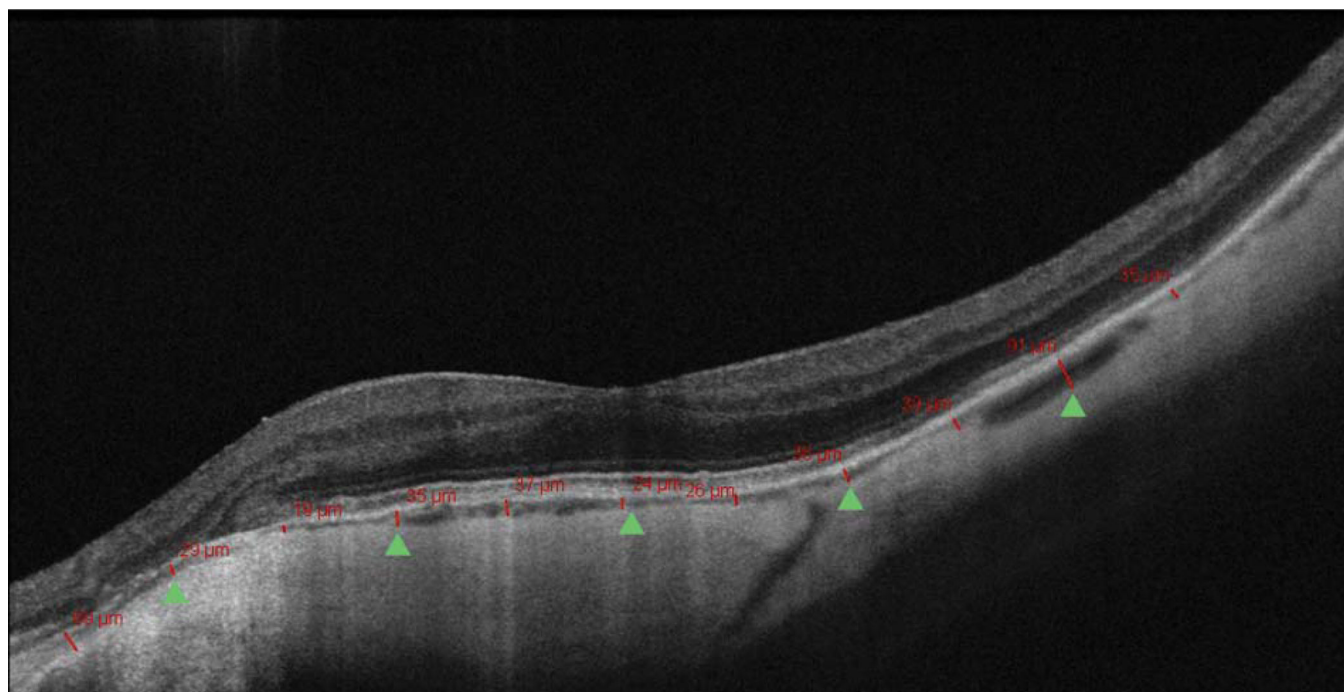


Fig. 7. Optical coherence tomography image of the choroid of a patient with high myopia taken on Cirrus HD-OCT (Carl Zeiss Meditec, Inc) with 20 images averaged. Note the choroid-sclera junction (green arrowhead). Choroidal thickness was measured in the fovea and at 500-μm intervals nasal and temporal to the fovea with the measurements expressed in micrometer (red lines). Note that the choroid is very thin.

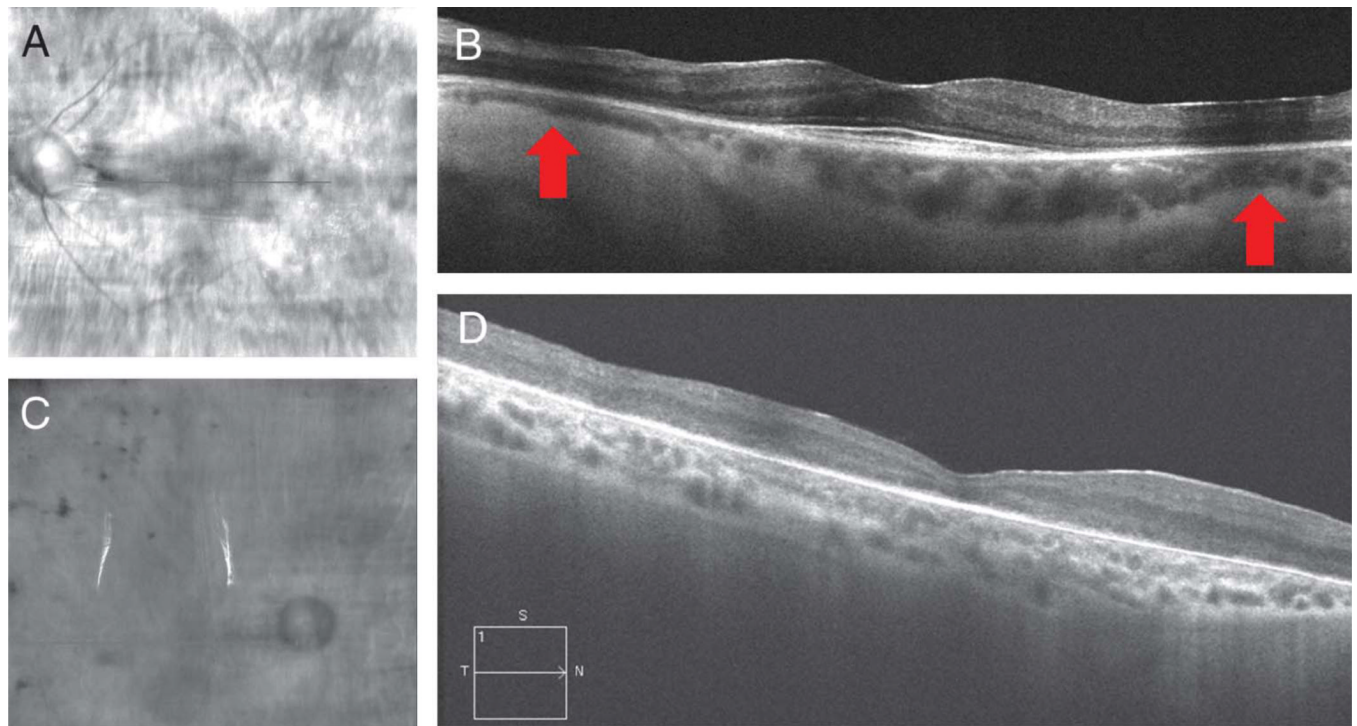


Fig. 8.

Optical coherence tomography image of the choroid of 2 patients with retinitis pigmentosa taken on Cirrus HD-OCT (Carl Zeiss Meditec, Inc) with 20 images averaged. **A.** OCT fundus image of the subject whose B-scan appears in **B**. Green line indicates location of the scan pattern on the fundus. **B.** B-scan of subject demonstrating focal thinning (red arrows) underneath areas of photoreceptor loss. **C.** Optical coherence tomographic fundus image of the subject whose B-scan appears in **D**. Green line indicates location of the scan pattern on the fundus. **D.** B-scan of subject demonstrating lack of choroidal thinning despite photoreceptor loss.

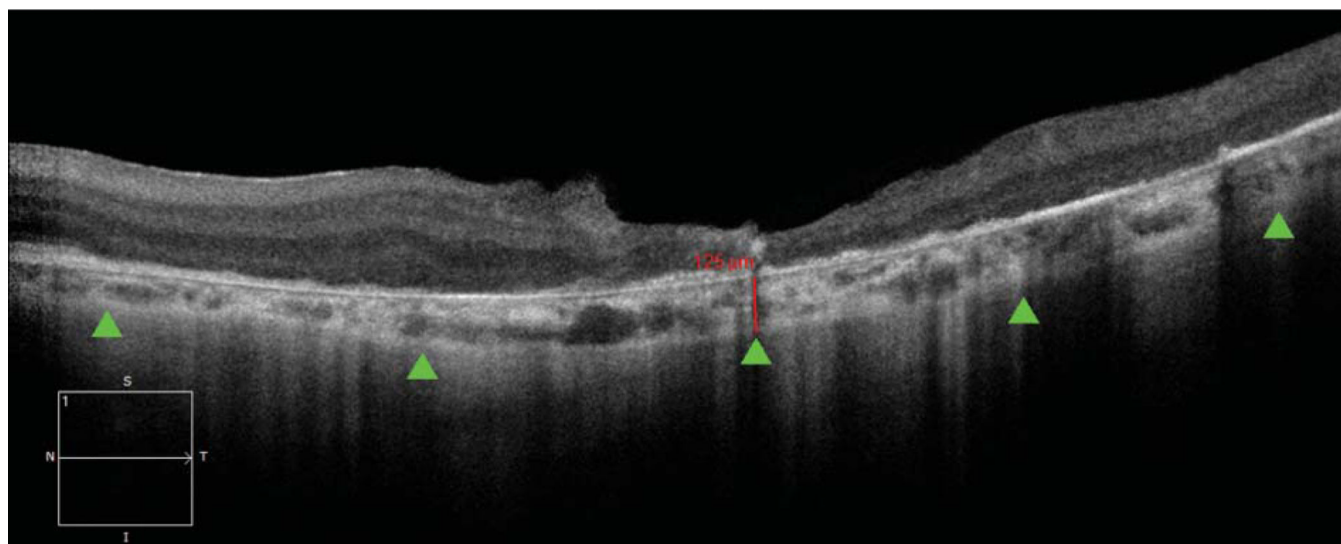


Fig. 9.

Optical coherence tomography image of the choroid of a patient with late phase of retinitis pigmentosa taken on Cirrus HD-OCT (Carl Zeiss Meditec, Inc) with 20 images averaged. Note that the choroid is thin (choroid sclera junction - green arrowhead). Choroidal thickness was measured in the fovea (red line). The choroid is hyperreflective due to the RPE atrophy.

Table 1

Chorioretinal Diseases With Changes in the Choroidal Thickness

Diseases With Thicker Choroid	Diseases With Thinner Choroid
Central serous retinopathy	Neovascular AMD
Polypoidal choroidal vasculopathy	Dry AMD
Vogt–Koenig–Harada	Proliferative diabetic retinopathy
	Diabetic macular edema
	Mutifocal choroiditis
	Retinitis pigmentosa
	Glaucoma